Gravitational waves in Einstein-æther and generalized TeVeS theory after GW170817

Yungui Gong (龚云贵),[†] Shaoqi Hou (侯绍齐),[*] and Dicong Liang (梁迪聪)[‡]
School of Physics, Huazhong University of Science and Technology, Wuhan, Hubei 430074, China

Eleftherios Papantonopoulos[§]
Department of Physics, National Technical University of Athens, Zografou Campus GR 157 73, Athens, Greece

(Received 17 January 2018; published 23 April 2018)

In this work we discuss the polarization contents of Einstein-æther theory and the generalized tensor-vector-scalar (TeVeS) theory, as both theories have a normalized timelike vector field. We derive the linearized equations of motion around the flat spacetime background using the gauge-invariant variables to easily separate physical degrees of freedom. We find the plane wave solutions and identify the polarizations by examining the geodesic deviation equations. We find that there are five polarizations in Einstein-æther theory and six polarizations in the generalized TeVeS theory. In particular, the transverse breathing mode is mixed with the pure longitudinal mode. We also discuss the experimental tests of the extra polarizations in Einstein-æther theory using pulsar timing arrays combined with the gravitational-wave speed bound derived from the observations on GW 170817 and GRB 170817A. It turns out that it might be difficult to use pulsar timing arrays to distinguish different polarizations in Einstein-æther theory. The same speed bound also forces one of the propagating modes in the generalized TeVeS theory to travel much faster than the speed of light. Since the strong coupling problem does not exist in some parameter subspaces, the generalized TeVeS theory is excluded in these parameter subspaces.

DOI: 10.1103/PhysRevD.97.084040

I. INTRODUCTION

The direct detection of gravitational waves (GWs) by the LIGO Scientific and Virgo collaborations marks the beginning of the era of testing general relativity (GR) in the strong-field regime [1–6]. In particular, the detection of GW170814 confirmed the polarization content of GWs for the first time, and the analysis showed that the pure tensor polarizations are favored against pure vector and pure scalar polarizations [4]. GW170817 was the first event of a binary neutron star merger. Together with its electromagnetic counterpart—the gamma-ray burst GRB 170817A [5,7,8]—they not only provided a very tight bound on the speed of GWs, but also heralded a new age of multimessenger astrophysics. While ground-based interferometers detect GWs in the high-frequency band (10–10^4 Hz), pulsar timing arrays (PTAs) [9–12] are sensitive to GWs in the lower-frequency band (around 10^{-10}–10^{-6} Hz) [13]. The intermediate-frequency band can be best probed by eLISA [14], TianQin [15], TaiJi, the DECi-hertz Interferometer Gravitational wave Observatory [16], and the recently proposed Mid-band Atomic Gravitational Wave Interferometric Sensor (MAGIS) [17]. So PTAs, eLISA, and MAGIS will provide tests of GWs that are complementary to LIGO/Virgo.

In general, GWs have at most six polarizations [18]. Alternative theories of gravity to GR predict extra polarizations, in addition to the familiar plus and cross polarizations in GR [19]. These extra polarizations are usually excited by the extra d.o.f. contained in alternative theories of gravity. For example, in scalar-tensor theories of gravity, the massless scalar field excites the transverse breathing polarization, while the massive one excites the longitudinal polarization [19–22]. More complicated alternative theories of gravity will add more polarizations, such as Einstein-æther theory [23,24] and the generalized tensor-vector-scalar (TeVeS) theory [25,26], whose GW polarization contents are the topics of the present work. Both theories have normalized timelike vector fields, which break the local Lorentz invariance (LLI). We will develop a gauge-invariant formalism to calculate the polarizations of GWs in modified gravitational theories like Einstein-æther theory and the generalized TeVeS theory, so that the physical d.o.f. are separated automatically, and GW solutions can be obtained in an arbitrary gauge. We will also present bounds

[*]Corresponding author.
shou1397@hust.edu.cn
[†]yggong@hust.edu.cn
[‡]dcliang@hust.edu.cn
[§]lpapa@central.ntua.gr

on the parameters respecting the recent observational results on GWs [5,7,8,27].

Einstein-æther theory is a local Lorentz-violating theory of gravity [23]. The gravitational interaction is mediated by the metric tensor $g_{\mu\nu}$ and a unit timelike vector field u^μ. Since u^μ never vanishes and pervades the Universe, it is called the "æther" field. It breaks LLI, as it defines a preferred frame everywhere in the spacetime. GW solutions have already been obtained in Ref. [24] in the flat spacetime background, where the æther field u^μ is at rest. It was found out that there are generally three extra polarizations, excited by the three d.o.f. of the æther field u^μ. Each polarization propagates at a speed different from 1 in a broad range of parameter space, although they are all massless. In the present work, GW solutions will be derived again using the gauge-invariant variables. The polarization contents of GWs are then discussed. With the recent bound on GW speed inferred from the observations of GW170817 and GRB 170817A [27], one sets bounds on the parameters in this theory, and thus predicts the possibility of detecting polarizations with PTAs by calculating the cross-correlation functions for different polarizations. The results show that the cross-correlation functions take very similar forms for different polarizations in some parameter regions, so it will be difficult to use PTAs to distinguish polarizations or to examine whether there are extra polarizations. However, there exist other parameter regions in which the cross-correlation functions vary a lot with different polarizations, which makes it possible to use PTAs to distinguish polarizations. The authors of Ref. [28] excluded generalized Einstein-æther theories [29] based on GW150914 [1].

TeVeS theory was originally proposed by Bekenstein to solve the dark matter problem [30]. It reduces to Milgrom's modified Newtonian dynamics (MOND) [31–33] in the nonrelativistic limit. In this theory, there are three fields mediating gravity: the "Einstein metric" tensor $g_{\mu\nu}$, a unit timelike vector field $\mathfrak{U}^\mu$, and a scalar field σ. Matter fields minimally couple to the physical metric which is related to the Einstein metric via the disformal transformation $\tilde{g}_{\mu\nu} = e^{-2\sigma} g_{\mu\nu} - 2\mathfrak{U}_\mu \mathfrak{U}_\nu \sinh(2\sigma)$. The action of $\mathfrak{U}^\mu$ is of Maxwellian type, a special form included in the æther's action. However, TeVeS theory suffers from some problems such as instability in the spherically symmetric solutions, and these problems could be cured by allowing the action of $\mathfrak{U}^\mu$ to be the most general one, i.e., that of the æther field [25]. The theory thus obtained is called the generalized TeVeS theory. Sagi has already discussed the GW solutions in the generalized TeVeS theory and its polarization content [26]. In the present work, the GW polarization content will be briefly analyzed again in a gauge-invariant way. We will also discuss the implications of the bound on the speed of GWs in this theory. The cosmological constraints on these alternative theories were discussed in Refs. [29,34,35].

This work is organized in the following way. First, in Sec. II we discuss the GW solutions around the flat spacetime background in Einstein-æther theory. In particular, after a brief introduction to Einstein-æther theory, we solve the equations of motion using the gauge-invariant variables in Sec. II A, and the polarization content of GWs is thus obtained in Sec. II B. We discuss the experimental constraints on Einstein-æther theory in Sec. II C. In Sec. II D, we compute the cross-correlation functions for different polarizations by taking into account the speed bound on GW propagation. Second, we discuss the GW solutions and the polarization content of the generalized TeVeS theory in Sec. III. Again, after a brief introduction, we obtain the GW solutions (mainly for the scalar field σ) and analyze the polarization content in Sec. III A. In Sec. III B we discuss the constraints on the generalized TeVeS theory. Finally, in Sec. IV we summarize our work. Throughout this work, we use units such that the speed of light in vacuum is $c = 1$.

II. GRAVITATIONAL WAVES IN EINSTEIN-ÆTHER THEORY

The action of Einstein-æther theory is given by [24]

$$S_{\text{EH-æ}} = \frac{1}{16\pi G}\int \mathrm{d}^4x\sqrt{-g}[R - c_1(\nabla_\mu u_\nu)\nabla^\mu u^\nu - c_2(\nabla_\mu u^\mu)^2 - c_3(\nabla_\mu u_\nu)\nabla^\nu u^\mu + c_4(u^\rho\nabla_\rho u^\mu)u^\sigma\nabla_\sigma u_\mu + \lambda(u^\mu u_\mu + 1)], \quad (1)$$

where λ is a Lagrange multiplier, G is the gravitational coupling constant, and the constants $c_i (i = 1, 2, 3, 4)$ are expected to be of the order unity. The Lagrange multiplier λ renders u^μ a normalized timelike vector field, which defines a preferred reference frame at each spacetime point. LLI is thus violated. Let $S_m[g_{\mu\nu}, \psi_m]$ be the matter action, where ψ_m collectively represents the matter fields. The field ψ_m is assumed to minimally couple with $g_{\mu\nu}$, so test particles follow geodesics in free fall. In the following section, the GW solutions will be obtained by expressing the linearized equations of motion in terms of the gauge-invariant variables.

A. Equations of motion

Ignoring the matter sector of the action, the equations of motion are obtained with the variational principle given below:

$$R_{\mu\nu} - \frac{1}{2}g_{\mu\nu}R = T^{\text{æ}}_{\mu\nu}, \quad (2)$$

$$c_1\nabla_\mu\nabla^\mu u_\nu + c_2\nabla_\nu\nabla_\mu u^\mu + c_3\nabla_\mu\nabla_\nu u^\mu - c_4\nabla_\mu(u^\mu a_\nu) + c_4 a_\mu\nabla_\nu u^\mu + \lambda u_\nu = 0, \quad (3)$$

$$u^\mu u_\mu + 1 = 0, \tag{4}$$

where $a^\mu = u^\nu \nabla_\nu u^\mu$ is the 4-acceleration of u^μ and the æther stress-energy tensor $T^{æ}_{\mu\nu}$ is

$$\begin{aligned} T^{æ}_{\mu\nu} = {} & \lambda\left[u_\mu u_\nu - \frac{1}{2} g_{\mu\nu}(u^\rho u_\rho + 1)\right] + c_1[(\nabla_\mu u_\rho)\nabla_\nu u^\rho - (\nabla_\rho u_\mu)\nabla^\rho u_\nu + \nabla_\rho(u_{(\mu}\nabla^\rho u_{\nu)} \\ & - u_{(\mu}\nabla_{\nu)}u^\rho + u^\rho \nabla_{(\mu}u_{\nu)})] + c_2 g_{\mu\nu}\nabla_\rho(u^\rho \nabla_\sigma u^\sigma) + c_3 \nabla_\rho(u_{(\mu}\nabla_{\nu)}u^\rho - u_{(\mu}\nabla^\rho u_{\nu)} \\ & + u^\rho \nabla_{(\mu}u_{\nu)}) + c_4[a_\mu a_\nu - \nabla_\rho(2u^\rho u_{(\mu}a_{\nu)} - a^\rho u_\mu u_\nu)] \\ & + \frac{1}{2} g_{\mu\nu}[-c_1(\nabla_\rho u_\sigma)\nabla^\rho u^\sigma - c_2(\nabla_\rho u^\rho)^2 - c_3(\nabla_\rho u_\sigma)\nabla^\sigma u^\rho + c_4 a_\rho a^\rho]. \end{aligned} \tag{5}$$

Here, Eq. (4) is a constraint equation.

In the following, we will look for GW solutions around the flat spacetime background, with the zeroth-order solution given by

$$g_{\mu\nu} = \eta_{\mu\nu}, \qquad u^\mu = \underline{u}^\mu = (1, 0, 0, 0). \tag{6}$$

Now, we perturb the metric and the æther field in the following way:

$$g_{\mu\nu} = \eta_{\mu\nu} + h_{\mu\nu}, \qquad u^\mu = \underline{u}^\mu + v^\mu. \tag{7}$$

We decompose the metric perturbation $h_{\mu\nu}$ and the perturbed æther field v^μ in the following way [36]:

$$h_{tt} = 2\phi, \tag{8}$$

$$h_{tj} = \beta_j + \partial_j \gamma, \tag{9}$$

$$h_{jk} = h^{\rm TT}_{jk} + \frac{1}{3} H \delta_{jk} + \partial_{(j}\epsilon_{k)} + \left(\partial_j\partial_k - \frac{1}{3}\delta_{jk}\nabla^2\right)\rho, \tag{10}$$

$$v^0 = \frac{1}{2} h_{00} = \phi, \tag{11}$$

$$v^j = \mu^j + \partial^j \omega. \tag{12}$$

In the above expressions, $h^{\rm TT}_{jk}$ is the transverse-traceless part of h_{jk}, satisfying $\partial^k h^{\rm TT}_{jk} = 0$ and $\eta^{jk} h^{\rm TT}_{jk} = 0$. β_j, ϵ_j, and μ^j are transverse vectors. Equation (11) is the consequence of $u^\mu u_\mu = -1$. Under the infinitesimal coordinate transformation $x^\mu \to x^\mu + \xi^\mu$, one has

$$h_{\mu\nu} \to h_{\mu\nu} - \partial_\mu \xi_\nu - \partial_\nu \xi_\mu, \tag{13}$$

$$u^\mu \to u^\mu + \underline{u}^\nu \partial_\nu \xi^\mu. \tag{14}$$

If an infinitesimal coordinate transformation is generated by $\xi_\mu = (\xi_t, \xi_j) = (A, B_j + \partial_j C)$ with $\partial^j B_j = 0$, it can be shown that [36]

$$\phi \to \phi - \dot{A}, \qquad \beta_j \to \beta_j - \dot{B}_j, \qquad \gamma \to \gamma - A - \dot{C}, \tag{15}$$

$$H \to H - 2\nabla^2 C, \quad \rho \to \rho - 2C, \quad \epsilon_j \to \epsilon_j - 2B_j, \tag{16}$$

$$h^{\rm TT}_{jk} \to h^{\rm TT}_{jk}, \tag{17}$$

where a dot denotes a partial time derivative and $\nabla^2 = \partial_j\partial^j$ is the Laplacian. The gauge transformation of the æther field is

$$\mu^j \to \mu^j + \dot{B}^j, \qquad \omega \to \omega + \dot{C}. \tag{18}$$

Therefore, gauge-invariant variables can be defined [36], which are $h^{\rm TT}_{jk}$ and

$$\Phi = -\phi + \dot{\gamma} - \frac{1}{2}\ddot{\rho}, \tag{19}$$

$$\Theta = \frac{1}{3}(H - \nabla^2 \rho), \tag{20}$$

$$\Xi_j = \beta_j - \frac{1}{2}\dot{\epsilon}_j, \tag{21}$$

$$\Sigma_j = \beta_j + \mu_j, \tag{22}$$

$$\Omega = \omega + \frac{1}{2}\dot{\rho}. \tag{23}$$

There are in total nine gauge-invariant variables. This is expected, as of the original fourteen variables the general covariance of the action (1) removes four d.o.f., and the constraint (4) removes one more. The equations of motion (2) and (3) will remove four more d.o.f., leaving five physical d.o.f.

After some straightforward but tedious algebraic manipulations, we get

$$\begin{aligned} & \frac{c_{14}}{2 - c_{14}}[c_{123}(1 + c_2 + c_{123}) - 2(1 + c_2)^2]\ddot{\Omega} \\ & \quad + c_{123}\nabla^2\Omega = 0, \end{aligned} \tag{24}$$

$$c_{14}\ddot{\Sigma}_j - \frac{c_1 - c_1^2/2 + c_3^2/2}{1 - c_{13}}\nabla^2\Sigma_j = 0, \tag{25}$$

$$\frac{1}{2}(c_{13} - 1)\ddot{h}^{\rm TT}_{jk} + \frac{1}{2}\nabla^2 h^{\rm TT}_{jk} = 0, \tag{26}$$

where $c_{13} = c_1 + c_3$, $c_{14} = c_1 + c_4$, and $c_{123} = c_1 + c_2 + c_3$. So there are only five propagating physical d.o.f. Two of them are tensor d.o.f. represented by $h^{\rm TT}_{jk}$, another two are vector d.o.f. given by Σ_j, and the remaining one is a scalar d.o.f. given by Ω. The squared speeds of these modes can be easily read off from the above equations, and they are

$$s_g^2 = \frac{1}{1 - c_{13}}, \tag{27}$$

$$s_v^2 = \frac{c_1 - c_1^2/2 + c_3^2/2}{c_{14}(1 - c_{13})}, \tag{28}$$

$$s_s^2 = \frac{c_{123}(2 - c_{14})}{c_{14}(1 - c_{13})(2 + 2c_2 + c_{123})}, \tag{29}$$

respectively. These speeds are generally different from one another and from 1. When $c_{13} = c_4 = 0$ and $2c_1c_2 = c_2 - c_1$ are satisfied, they are simultaneously one. The remaining gauge-invariant variables are given by

$$\Phi = \frac{c_{14} - 2c_{13}}{2 - c_{14}}\dot{\Omega}, \tag{30}$$

$$\Theta = \frac{2c_{14}(c_{13} - 1)}{2 - c_{14}}\dot{\Omega}, \tag{31}$$

$$\Xi_j = -\frac{c_{13}}{1 - c_{13}}\Sigma_j. \tag{32}$$

These are dependent variables. In deriving these relations, one imposes the following conditions:

$$c_{13} \neq 1, \quad c_{14} \neq 0, \quad c_{14} \neq 2, \quad 3c_2 \neq -2 - c_{13}. \tag{33}$$

B. Polarizations of gravitational waves

Since the matter fields are assumed to minimally couple with the metric tensor only, the polarization content of GWs in Einstein-æther theory is determined by examining the linearized geodesic deviation equation

$$\ddot{x}^j = \frac{d^2x^j}{dt^2} = -R_{tjtk}x^k, \tag{34}$$

which describes the relative acceleration between two nearby test particles separated by the deviation vector x^j. In terms of gauge-invariant variables, the electric components R_{tjtk} of the Riemann tensor are given by [36]

$$R_{tjtk} = -\frac{1}{2}\ddot{h}^{\rm TT}_{jk} + \dot{\Xi}_{(j,k)} + \Phi_{,jk} - \frac{1}{2}\ddot{\Theta}\delta_{jk}. \tag{35}$$

To be more specific and due to the rotational symmetry of the Minkowski spacetime, one considers a situation where the plane GWs propagate in the $+z$ direction. The wave vectors of the scalar, vector, and tensor modes are

$$k_s^\mu = \omega_s(1, 0, 0, 1/s_s), \tag{36}$$

$$k_v^\mu = \omega_v(1, 0, 0, 1/s_v), \tag{37}$$

$$k_g^\mu = \omega_g(1, 0, 0, 1/s_g), \tag{38}$$

respectively, where the ω's are the corresponding angular frequencies. In this case, the nonvanishing components of $h^{\rm TT}_{jk}$ are $h^{\rm TT}_{11} = -h^{\rm TT}_{22} = h_+$ and $h^{\rm TT}_{12} = h^{\rm TT}_{21} = h_\times$. For the vector mode, $\Sigma_3 = 0$ since $\partial_j\Sigma^j = 0$.

By calculating R_{tjtk} we find that there are five polarization states. In terms of R_{tjtk}, the plus polarization is given by $\hat{P}_+ = -R_{txtx} + R_{tyty} = \ddot{h}_+$, and the cross polarization is $\hat{P}_\times = R_{txty} = -\ddot{h}_\times$; the vector-$x$ polarization is represented by $\hat{P}_{xz} = R_{txtz} = -c_{13}\partial_3\dot{\Sigma}_1/[2(1 - c_{13})]$, and the vector-$y$ polarization is $\hat{P}_{yz} = R_{txty} = -c_{13}\partial_3\dot{\Sigma}_2/[2(1 - c_{13})]$; the transverse breathing polarization is specified by $\hat{P}_b = R_{txtx} + R_{tyty} = -2c_{14}(c_{13} - 1)\dddot{\Omega}/(2 - c_{14})$, and the longitudinal polarization is

$$\begin{aligned}\hat{P}_l = R_{tztz} &= \frac{c_{14} - 2c_{13}}{2 - c_{14}}\partial_3^2\dot{\Omega} - \frac{c_{14}(c_{13} - 1)}{2 - c_{14}}\dddot{\Omega} \\ &= \left[\frac{c_{14} - 2c_{13}}{2 - c_{14}}\frac{1}{s_s^2} - \frac{c_{14}(c_{13} - 1)}{2 - c_{14}}\right]\dddot{\Omega}.\end{aligned}$$

Among these polarizations, both the transverse breathing and the longitudinal modes are excited by the scalar d.o.f. Ω, so Ω excites a mixed state of $\hat{P}_b$ and $\hat{P}_l$, as in the case of Horndeski theory [21,22]. One can also calculate the Newman-Penrose variables [18,37,38], and it is found that none of them vanish in general.

In the following discussion, the gauge will be fixed so that

$$h_{0j} = 0, \qquad v^j{}_{,j} = 0, \tag{39}$$

which implies that $\Sigma_j = \mu_j = v_j$ and $\dot{\Omega} = \frac{2 - c_{14}}{2(c_{13} - 1)}\dot{\phi}$. Therefore, one obtains

$$h_+ = e_+\cos[\omega_g(t - z/s_g)], \tag{40}$$

$$h_\times = e_\times\cos[\omega_g(t - z/s_g)], \tag{41}$$

$$v_j = \mu_j^0\cos[\omega_v(t - z/s_v)], \quad j = 1, 2, \tag{42}$$

$$\phi = \varphi\cos[\omega_g(t - z/s_s)], \tag{43}$$

where e_+, $e_\times$, μ_j^0, and φ are the amplitudes.

C. Discussion on the constraints

As mentioned before, LLI is violated. This can be seen in the post-Newtonian formalism developed by Foster and Jacobson [39]. The post-Newtonian parameters α_1 and α_2 are given by

$$\alpha_1 = -\frac{8(c_3^2 + c_1 c_4)}{2c_1 - c_1^2 + c_3^2}, \tag{44}$$

$$\alpha_2 = \frac{(2c_{13} - c_{14})^2}{c_{123}(2 - c_{14})} - \frac{12c_3 c_{13} + 2c_1 c_{14}(1 - 2c_{14}) + (c_1^2 - c_3^2)(4 - 6c_{13} + 7c_{14})}{(2 - c_{14})(2c_1 - c_1^2 + c_3^2)}. \tag{45}$$

These parameters together with α_3 (which vanishes in Einstein-æther theory) measure the preferred-frame effects at the post-Newtonian order [40]. According to Ref. [19], $|\alpha_1| \lesssim 10^{-4}$ from the Lunar Laser Ranging experiments, and $|\alpha_1| \lesssim 4 \times 10^{-5}$ based on the observation of PSR J1738 + 0333 [41]. In addition, $|\alpha_2| \lesssim 2 \times 10^{-9}$ was obtained using the observations of the millisecond pulsars B1937 + 21 and J1744-1134 [42,43].

Moreover, Newton's constant is found to be [39,44]

$$G_{\rm N} = \frac{G}{1 - c_{14}/2}, \tag{46}$$

and the gravitational constant appearing in the Friedman equation is [44]

$$G_{\rm cosmo} = \frac{G}{1 + (c_{13} + 3c_2)/2}. \tag{47}$$

In contrast to GR, these two constants are not the same, so the expansion rate of the Universe is different from that predicted by GR even if the matter content is the same in the two theories. Thus the ratio of the two constants should be constrained, for example, by the observed primordial ^{4}He abundance [44],

$$\left| \frac{G_{\rm cosmo}}{G_{\rm N}} - 1 \right| < \frac{1}{8}. \tag{48}$$

The energy carried away by the gravitational waves should be positive, which leads to the following conditions [45]:

$$\frac{2c_1 - c_1^2 + c_3^2}{1 - c_{13}} > 0, \tag{49}$$

$$c_{14}(2 - c_{14}) > 0. \tag{50}$$

Finally, all of the speeds (27)–(29) should be greater than 1 so that there is no gravitational Cherenkov radiation [46].

The recent observation of GW170817 [5] determined that photons arrived at the Earth about 1.7 s later than the GWs, which has been used to set bounds on GWs' speed [27],

$$-3 \times 10^{-15} \le \frac{v_{\rm GW} - v_{\rm EM}}{v_{\rm EM}} \le 7 \times 10^{-16}, \tag{51}$$

where $v_{\rm GW}$ and $v_{\rm EM}$ are the speeds of the GW and the photon, respectively. Suppose the photon speed $v_{\rm EM}$ is 1; then, the GW speed is bounded from above, i.e., $v_{\rm GW} \le 1 + 7 \times 10^{-16}$. If the detected GW signal is a tensor wave, then one obtains

$$c_{13} \le 1.4 \times 10^{-15} \tag{52}$$

using the speed squared for the spin-2 graviton $s_g^2 = 1/(1 - c_{13})$.

Combining all of the constraints listed above, one can set bounds on the c_i's. Because α_1 and α_2 are constrained to be small by observations, one can expand the theory in powers of α_1 and α_2 [47,48]. At the leading order

$$c_2 = \frac{c_{13}(c_3 - 2c_1)}{3c_1}, \tag{53}$$

$$c_4 = -\frac{c_3^2}{c_1}, \tag{54}$$

by setting α_1 and α_2 to zero. Although at this order the α's all vanish, the preferred-frame effects will show up at higher orders in α_1 and α_2. Even if the α's vanish identically, LLI is still violated as the α's only parametrize the violation of LLI at the post-Newtonian order. Now, the parameter space reduces to two dimensions, and it is parametrized by $c_\pm = c_1 \pm c_3$, with $c_+ = c_{13}$. The parameters $c_\pm$ are constrained by the requirements that the perturbation around the flat spacetime background is stable and has positive energy [24], and that there is no gravitational Cherenkov radiation [46]. These leads to

$$0 \le c_+ \le 1, \qquad 0 \le c_- \le \frac{c_+}{3(1 - c_+)} \tag{55}$$

to the leading order in α_1 and α_2. These constraints lead to the superluminal propagation of GWs in the flat spacetime background [24].

Yagi *et al.* [47,48] put further constraints on $c_\pm$ from binary pulsar observations. Together with the stability and no-Cherenkov-radiation requirements, the binary pulsar observations have pushed the available parameter space (c_+, c_-) to a small corner, as shown in Fig. 1 in Ref. [48]. Let c_+ saturate the bound (52), i.e., $c_+ = 1.4 \times 10^{-15}$, so $s_g = 1 + 7 \times 10^{-16}$. A careful examination of Fig. 1 in Ref. [48] shows that $c_- \lesssim 0.32 c_+$ and $c_+ \lesssim 0.005$. For future computations we choose the parametrization

$$c_- = r_- c_+ \tag{56}$$

near $c_+ = 1.4 \times 10^{-15}$ with $r_- \lesssim 0.32$. Then, by using the speeds of the vector and scalar GWs discussed in the previous subsection, we obtain

$$s_v = \frac{1}{2}\sqrt{\frac{(1+r_-)(1+r_- - r_- c_+)}{r_-}}\, s_g, \tag{57}$$

$$s_s = \frac{s_g}{\sqrt{3 r_-}}. \tag{58}$$

If $r_- = 0.1$, 0.2, or 0.3, one gets three sets of speeds, which are listed in Table I. As it shows, all speeds exceed 1 and decrease with r_-. One can also check that with the chosen r_-, all c_i's are of the order of 10^{-15}. The smallness of these parameters requires severe fine-tuning.

One may also let $c_{13} = 0$ without setting $\alpha_1 = \alpha_2 = 0$, as done in Ref. [49]. In this case, $s_g = 1$, i.e., the tensor GW propagates at the exact speed of light, and

$$s_v^2 = \frac{c_1}{c_{14}}, \qquad s_s^2 = \frac{c_2(2 - c_{14})}{c_{14}(2 + 3c_2)}. \tag{59}$$

In addition, α_1 and α_2 reduce to

$$\alpha_1 = -4c_{14}, \qquad \alpha_2 = \frac{c_{14}[c_2 - c_{14}(1 + 2c_2)]}{c_2(c_{14} - 2)}. \tag{60}$$

Using the constraints on s_v, s_s, α_1, and α_2 together with the inequalities (48)–(50), one concludes that

$$c_1 = -c_3 > 0, \qquad 0 < c_{14} < 10^{-5}. \tag{61}$$

The constraints on c_2 are more complicated, and are given by

$$\frac{c_{14}}{1 - 2c_{14}} < c_2 < c_2^u(c_{14}), \tag{62}$$

where the upper bound is defined as

$$c_2^u(c_{14}) = \begin{cases} \frac{2(1-4c_{14})}{21}, & 0 < c_{14} \lesssim 4 \times 10^{-9}, \\ \frac{c_{14}}{1 - 2c_{14} - 2\times 10^{-9}\frac{(2-c_{14})}{c_{14}}}, & 4 \times 10^{-9} \lesssim c_{14} < 10^{-5}. \end{cases} \tag{63}$$

Figure 1 shows the constraints on c_2 in the range $(0 < c_{14} < 8 \times 10^{-9})$, and the shaded region is allowed.

TABLE I. The speeds of the vector and scalar GWs.

r_-	0.1	0.2	0.3
s_v	1.74	1.34	1.19
s_s	1.83	1.29	1.05

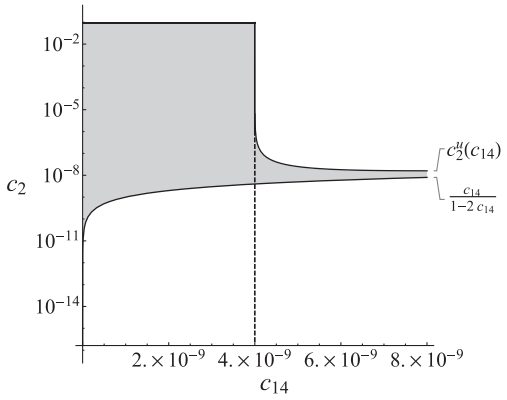

FIG. 1. The constraints on c_2 in the range $0 < c_{14} < 8 \times 10^{-9}$. The shaded region is allowed. As c_{14} increases the upper and the lower bounds approach each other. Note that the vertical axis uses a logarithmic scale.

As c_{14} increases the upper and the lower bounds approach each other. The bounds on c_2 and c_{14} are different from those in Ref. [49] since they used different values for the constraints, such as $|\alpha_1| \leq 10^{-4}$ and $|\alpha_2| \leq 10^{-7}$. Table II shows the possible choices for the c_i's such that each column reproduces the corresponding column in Table I. These c_i's are of the order of 10^{-9}, which might still require fine-tuning, albeit less than when setting $\alpha_1 = \alpha_2 = 0$ and $c_+ = 1.4 \times 10^{-15}$. Note that when $c_{13} = 0$, the vector polarizations disappear.

D. Pulsar timing arrays

A pulsar is a rotating neutron star or a white dwarf with a very strong magnetic field. It emits a beam of electromagnetic radiation at a steady rate, and millisecond pulsars can be used as stable clocks [50]. The presence of GWs will alter the rate, because they will affect the propagation time of the radiation. This will lead to a change in the time of arrival (TOA), called the timing residual $R(t)$. Timing residuals are correlated between widely separated pulsars, and the function $C(\theta) = \langle R_a(t) R_b(t) \rangle$ is used to measure this correlation, where θ is the angular separation of pulsars a and b, and the brackets $\langle\rangle$ indicate the ensemble average over the stochastic GW background. This underlies the detection of GWs and the probe of the polarization content.

TABLE II. The possible choices for the c_i's to reproduce the speeds in Table I. The last two rows are the speeds of the vector and scalar GWs determined by the choices made in the first three rows. The c_i's are normalized by 10^{-9}.

$c_1 = -c_3$	6.06	3.59	2.83
c_2	3.66	2.58	2.10
c_4	−4.06	−1.59	−0.83
s_v	1.74	1.34	1.19
s_s	1.83	1.29	1.05

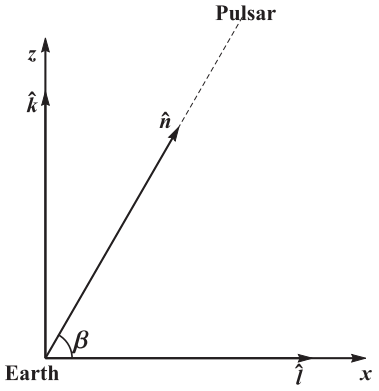

FIG. 2. The GW propagates in the direction $\hat{k}$ and the photon travels in the $-\hat{n}$ direction at the leading order. $\hat{l}$ is perpendicular to $\hat{k}$ and in the same plane determined by $\hat{k}$ and $\hat{n}$. The angle between $\hat{n}$ and $\hat{l}$ is β.

The authors of Refs. [51–53] considered the effects of GWs in GR on the timing residuals for the first time. Hellings and Downs proposed a method to detect the effects by cross-correlating the time derivatives of the timing residuals between pulsars [54], while Jenet *et. al.* directly used the timing residuals instead of the time derivative [55]. The generalization to massless GWs in alternative metric theories of gravity was soon done in Ref. [56], and further to massive GWs in Refs. [57,58]. For more work on PTAs, please refer to Refs. [59–62] and references therein.

In order to calculate the timing residual $R(t)$ caused by the GW solution (40)–(43), one sets up a coordinate system as shown in Fig. 2. In this coordinate system, the Earth is at the origin and the distant pulsar is assumed to be stationary at $x_p = (L\cos\beta, 0, L\sin\beta)$, when there is no GW. The GW propagates in the direction $\hat{k} = (0,0,1)$, and $\hat{n}$ is the unit vector pointing from the Earth to the pulsar. Let $\hat{l} = \hat{k} \wedge (\hat{n} \wedge \hat{k})/\cos\beta = [\hat{n} - \hat{k}(\hat{n}\cdot\hat{k})]/\cos\beta$ be the unit vector parallel to the y axis. At the leading order, i.e., in the absence of GWs, the photon travels at a 4-velocity $\underline{u}^\mu = \gamma_0(1, -\cos\beta, 0, -\sin\beta)$, where $\gamma_0 = \mathrm{d}t/\mathrm{d}\lambda$ is a constant and λ is an arbitrary affine parameter. The perturbed photon 4-velocity is $u^\mu = \underline{u}^\mu + V^\mu$. The photon geodesic equation is

$$0 = \frac{\mathrm{d}u^\mu}{\mathrm{d}\lambda} + \Gamma^\mu{}_{\rho\sigma}u^\rho u^\sigma \approx \gamma_0\frac{\mathrm{d}V^\mu}{\mathrm{d}t} + \Gamma^\mu{}_{\rho\sigma}\underline{u}^\rho\underline{u}^\sigma. \quad (64)$$

Solving it gives the perturbation in the photon 4-velocity, which is too complicated and will not be reproduced here.

Next, we calculate the 4-velocities of the Earth and the pulsar. First, we calculate the 4-velocity of the pulsar, which is supposed to be $u_p^\mu = u_p^0(1, \vec{v}_p)$. The geodesic equation for the pulsar is

$$\begin{aligned} 0 &= \frac{\mathrm{d}^2x^\mu}{\mathrm{d}\tau^2} + \Gamma^\mu{}_{\rho\nu}\frac{\mathrm{d}x^\rho}{\mathrm{d}\tau}\frac{\mathrm{d}x^\nu}{\mathrm{d}\tau} \\ &\approx (u_p^0)^2\left(\frac{\mathrm{d}^2x^\mu}{\mathrm{d}t^2} + \Gamma^\mu{}_{00}\right) + u_p^0\frac{\mathrm{d}u_p^0}{\mathrm{d}t}\frac{\mathrm{d}x^\mu}{\mathrm{d}t}, \end{aligned} \quad (65)$$

where τ is the proper time. One sets $x = L\cos\beta$ and $y = 0$. Therefore, the 4-velocity of an observer at rest at the pulsar is

$$\begin{aligned} u_p^\mu = \Bigg(&1 + \varphi\cos\omega_s\left(t - \frac{L}{s_s}\cos\beta\right), 0, 0, \\ &-\frac{\varphi}{s_s}\cos\omega_s\left(t - \frac{L}{s_s}\cos\beta\right)\Bigg). \end{aligned} \quad (66)$$

To get the 4-velocity of an observer at rest at the Earth we simply set $L = 0$ in the above expression, so

$$u_e^\mu = \left(1 + \varphi\cos\omega_s t, 0, 0, -\frac{\varphi}{s_s}\cos\omega_s t\right). \quad (67)$$

Note that although Einstein-æther theory contains five d.o.f., the velocities of observers (initially at rest) only depend on the scalar d.o.f. ϕ. In contrast, the photon's 4-velocity also depends on the tensor and vector d.o.f.

The frequencies measured by the observer at the Earth and by the one at the pulsar are $f_r = -u_\mu u_e^\mu$ and $f_e = -u_\mu u_p^\mu$, respectively. The relative frequency shift is thus

$$\begin{aligned} \frac{f_e - f_r}{f_r} =& \frac{(c_{14} - 2c_{13})(\hat{k}\cdot\hat{n})^2 + s_s^2c_{14}(1 - c_{13})}{2(1 - c_{13})s_s(s_s + \hat{k}\cdot\hat{n})}[\phi(t,0) - \phi(t - L/s_s, L\hat{n})] \\ &- \frac{c_{13}\hat{k}\cdot\hat{n}}{(1 - c_{13})(s_v + \hat{k}\cdot\hat{n})}[\hat{n}\cdot\vec{v}(t,0) - \hat{n}\cdot\vec{v}(t - L/s_v, L\hat{n})] + \frac{s_g\hat{n}^j\hat{n}^k}{2(s_g + \hat{k}\cdot\hat{n})}[h_{jk}^{\mathrm{TT}}(t,0) - h_{jk}^{\mathrm{TT}}(t - L/s_g, L\hat{n})]. \end{aligned} \quad (68)$$

This has been put in a coordinate-free form so that this formula always applies regardless of the direction of GW propagation. The second and last lines both agree with the results in Ref. [56] when $s_g = s_v = 1$. The contribution of the scalar polarization (the first line) does not reduce to the results in Refs. [21,22] in a straightforward way where GWs in Horndeski theory are considered, as the scalar fields interact rather differently in these two theories.

In the above discussion, each propagating mode was taken to be monochromatic. In reality, the stochastic GW background can be described by

$$\phi(t,\vec{x}) = \int_{-\infty}^{\infty} \frac{\mathrm{d}\omega}{2\pi} \int \mathrm{d}^2\hat{k}\{\varphi(\omega,\hat{k}) \exp[i(\omega t - k\hat{k}\cdot\vec{x})]\}, \tag{69}$$

$$\vec{v}(t,\vec{x}) = \int_{-\infty}^{\infty} \frac{\mathrm{d}\omega}{2\pi} \int \mathrm{d}^2\hat{k}\{\vec{\mu}(\omega,\hat{k}) \exp[i(\omega t - k\hat{k}\cdot\vec{x})]\}, \tag{70}$$

$$h_{jk}^{\mathrm{TT}}(t,\vec{x}) = \sum_{P=+,\times} \int_{-\infty}^{\infty} \frac{\mathrm{d}\omega}{2\pi} \times \int \mathrm{d}^2\hat{k}\{\epsilon_{jk}^{P} h_P(\omega,\hat{k}) \exp[i(\omega t - k\hat{k}\cdot\vec{x})]\}, \tag{71}$$

where $\varphi(\omega,\hat{k})$, $\vec{\mu}(\omega,\hat{k})$, and $h_P(\omega,\hat{k})$ are the amplitudes of the scalar, vector, and tensor GWs oscillating at ω and propagating in the direction $\hat{k}$, respectively. ϵ_{jk}^{P} is the polarization matrix and $P = +,\times$. $\vec{\mu}(\omega,\hat{k})$ is transverse, i.e., $\hat{k}\cdot\vec{\mu} = 0$. So if the unit vectors $\hat{e}_{\bar{1}}$, $\hat{e}_{\bar{2}}$, and $\hat{e}_{\bar{3}} = \hat{k}$ form a triad such that $\hat{e}_{\bar{j}}\cdot\hat{e}_{\bar{l}} = \delta_{\bar{j}\bar{l}}$, and $\hat{e}_{\bar{3}} = \hat{e}_{\bar{1}}\times\hat{e}_{\bar{2}}$, then $\vec{\mu}(\omega,\hat{k})$ has two d.o.f., which can be expressed as

$$\vec{\mu}(\omega,\hat{k}) = \hat{e}_{\bar{1}}\mu_{\bar{1}}(\omega,\hat{k}) + \hat{e}_{\bar{2}}\mu_{\bar{2}}(\omega,\hat{k}). \tag{72}$$

Integrating the relative frequency shift gives the timing residual

$$R(T) = \int_{-\infty}^{\infty} \frac{\mathrm{d}\omega}{2\pi} \int \mathrm{d}^2\hat{k} \int_0^T \mathrm{d}t \frac{f_e - f_r}{f_r}, \tag{73}$$

where the argument T is the total observation time. Suppose that the stochastic GW background is isotropic, stationary, and independently polarized; then, one defines the characteristic strains $\varphi_c(\omega)$, $\mu_{\bar{j}}^{c}(\omega)$, and $h_c^P(\omega)$ in the following manner:

$$\langle\varphi^*(\omega,\hat{k})\varphi(\omega',\hat{k}')\rangle = \delta(\omega-\omega')\delta^{(2)}(\hat{k}-\hat{k}')\frac{|\varphi_c(\omega)|^2}{\omega}, \tag{74}$$

$$\langle\mu_{\bar{j}}^{*}(\omega,\hat{k})\mu_{\bar{l}}(\omega',\hat{k}')\rangle = \delta(\omega-\omega')\delta^{(2)}(\hat{k}-\hat{k}')\delta_{\bar{j}\bar{l}}\frac{|\mu_{\bar{j}}^{c}(\omega)|^2}{\omega}, \tag{75}$$

$$\langle h_P^{*}(\omega,\hat{k})h_P(\omega',\hat{k}')\rangle = \delta(\omega-\omega')\delta^{(2)}(\hat{k}-\hat{k}')\delta^{PP'}\frac{\pi|h_c^P(\omega)|^2}{4\omega}, \tag{76}$$

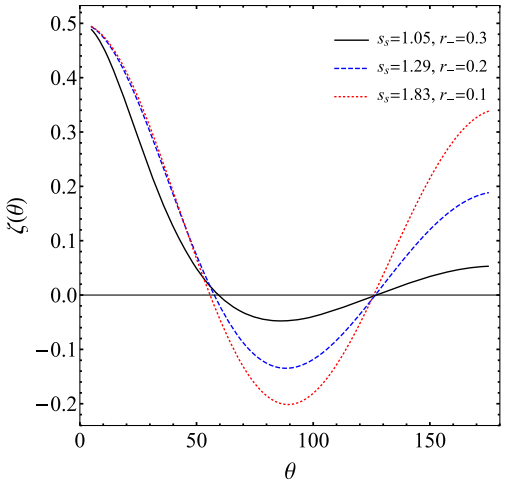

FIG. 3. The normalized cross correlation $\zeta(\theta) = C_s(\theta)/C_s(0)$ for the scalar GW. $\zeta(\theta)$ is plotted for different propagation speeds corresponding to different r_- [see Eq. (56)].

where a star $*$ indicates complex conjugation. The characteristic strains are proportional to ω^{α}, where α is the power-law index. The cross-correlation function $C(\theta) = \langle R_a(T)R_b(T)\rangle$ can thus be obtained. The detailed calculation has been relegated to the Appendix. The normalized cross correlation $\zeta(\theta) = C(\theta)/C(0)$ is calculated numerically, and the results are shown in Figs. 3, 4, and 5 for the scalar, vector, and tensor polarizations, respectively.

Figure 3 shows the behavior of $\zeta(\theta)$ as a function of θ at different speeds s_s, corresponding to different r_- [see Eq. (56)] for the scalar polarization. As one can see, $\zeta(\theta)$ increases with θ in the small- and large-angle ranges, while it decreases in the intermediate-angle range. It becomes negative in certain ranges. The inspection of the dependence of $\zeta(\theta)$ on s_s or r_- shows that $\zeta(\theta)$ is more sensitive to s_s or r_- when θ is large. As discussed in

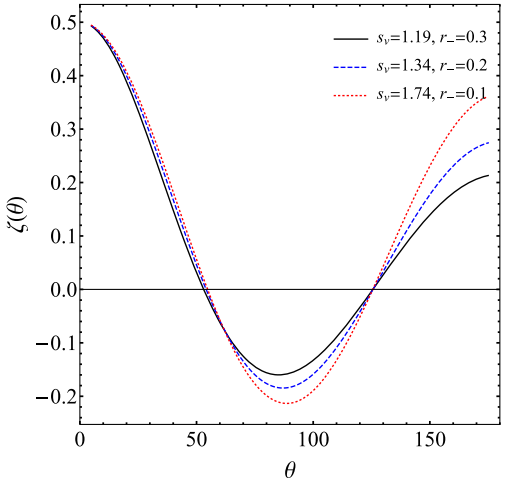

FIG. 4. The normalized cross correlation $\zeta(\theta) = C_v(\theta)/C_v(0)$ for the vector GW. $\zeta(\theta)$ is plotted for different propagation speeds corresponding to different f's [see Eq. (56)].

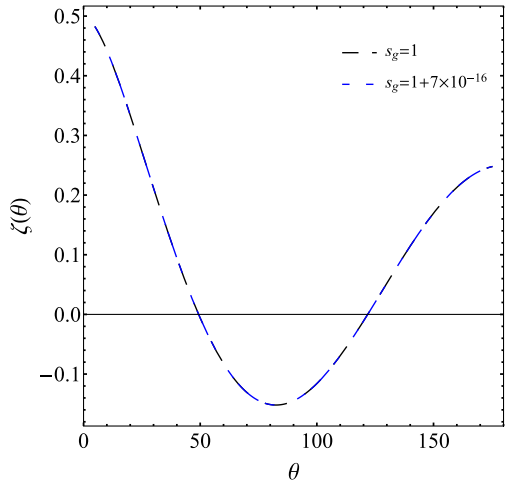

FIG. 5. The normalized cross correlation $\zeta(\theta) = C_g(\theta)/C_g(0)$ for the tensor GW at $s_g = 1 + 7 \times 10^{-16}$. Also shown is $\zeta(\theta)$ for GR ($s_g = 1$). Since the difference in the speeds is extremely small, the two curves nearly overlap with each other.

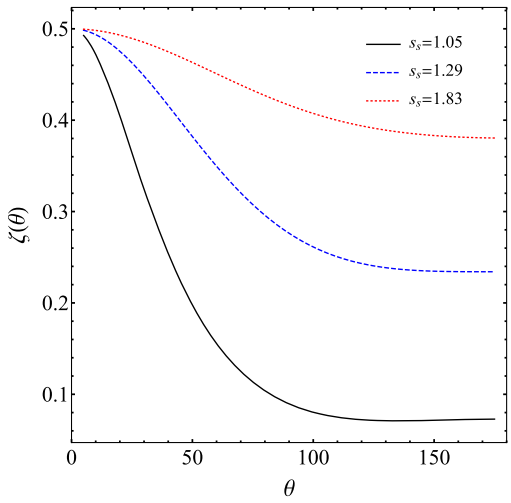

FIG. 6. The normalized cross-correlation function $\zeta(\theta) = C_s(\theta)/C_s(0)$ for the scalar GW when the c_i's take the values in Table II.

the Appendix, $\zeta(\theta)$ does not depend on the power-law index α. The behavior of $\zeta(\theta)$ in this work differs greatly from that for the scalar GWs in the scalar-tensor theory obtained in Refs. [21,22], where $\zeta(\theta)$ for the scalar GWs in Horndeski theory was obtained for different masses and the power-law index α, and it is always positive and a decreasing function of θ [21]. The behavior of $\zeta(\theta)$ in this work is also different from that for the transverse breathing and longitudinal polarizations presented in Refs. [56–58], where these two polarizations were treated as independent of each other.

Figure 4 shows how $\zeta(\theta)$ varies as a function of θ at different s_v or r_- for the vector polarizations. One finds that $\zeta(\theta)$ also has similar behavior as that for the scalar GWs and it does not depend on the power-law index α, but it is not as sensitive to s_v or r_- as the one for the scalar GWs. Comparing this figure with the bottom-left panel in Fig. 1 in Ref. [56] shows that $\zeta(\theta)$ becomes flatter at large angles in Ref. [56]. $\zeta(\theta)$ for the massive GWs was considered in Ref. [58], and the bottom-left panel in Fig. 1 in Ref. [58] is for the vector polarizations. They show some similarities to the one in the current work.

Figure 5 shows $\zeta(\theta)$ for the tensor polarizations at $s_g = 1 + 7 \times 10^{-16}$. Also shown is the one for GR labeled by $s_g = 1$, which is given by [54,56]

$$\zeta(\theta) = \frac{3}{4}(1-\cos\theta)\ln\frac{1-\cos\theta}{2} + \frac{1}{2} - \frac{1-\cos\theta}{8} + \frac{\delta(\theta)}{2}. \tag{77}$$

Since the difference in the speeds is extremely small, the two curves nearly overlap with each other.

If one chooses the values for the c_i's given in Table II, the normalized cross-correlation function $\zeta(\theta)$ for the scalar GW is modified, as shown in Fig. 6. $\zeta(\theta)$ for the tensor GW is described by the curve labeled by "$s_g = 1$" in Fig. 5. Since when $c_{13} = 0$ the vector polarizations disappear, we do not plot the corresponding cross-correlation functions. It is clear that $\zeta(\theta)$ for the scalar GW behaves rather differently than the one for the tensor GW.

Finally, let us compare the cross-correlation functions for the scalar, vector, and tensor polarizations in Einstein-æther theory. If one chooses the c_i's to make $\alpha_1 = \alpha_2 = 0$, the cross-correlation functions for the vector modes are quite similar to those for the tensor modes with a small variation depending on the speed s_v, as shown in Figs. 3, 4, and 5. The cross-correlation function for the scalar mode is somewhat different than those for the vector and the tensor modes when its speed is small, for example, $s_s = 1.05$ (the black curve in Fig. 3), but when its speed is larger the difference becomes smaller. Compared to the results in Refs. [21,56–58], Figs. 3, 4, and 5 show greater similarities among the cross-correlation functions for different polarizations, so it is more difficult to use PTAs to distinguish different polarizations and thus test whether extra polarizations exist in Einstein-æther theory. However, if one chooses the c_i's to make $s_g = 1$ (i.e., the values in Table II), there is only one extra polarization state, and its cross-correlation function differs from that of the tensor modes greatly. So it would be easier to use PTAs to distinguish different polarizations in Einstein-æther theory, and thus falsify it if no extra polarization is observed.

III. GRAVITATIONAL WAVES IN THE GENERALIZED TeVeS THEORY

The action of the generalized TeVeS theory is given by the sum of that of Einstein-æther theory (1) and the one for the additional scalar field σ,

$$S_\sigma = -\frac{8\pi}{\jmath^2\ell^2 G}\int \mathrm{d}^4x\sqrt{-g}\mathcal{F}(\jmath\ell^2 j^{\mu\nu}\sigma_{,\mu}\sigma_{,\nu}), \quad (78)$$

where $j^{\mu\nu} = g^{\mu\nu} - u^\mu u^\nu$, $\jmath$ is a dimensionless positive parameter, and ℓ is a constant with dimensions of length. The function $\mathcal{F}$ is dimensionless and chosen to produce the relativistic MOND phenomena. Here, since the action of the vector field is that of the æther, we simply use u^μ to represent $\mathfrak{U}^\mu$.

Because of the extra scalar field σ, the equations of motion (2) and (3) are modified. First, on the right-hand side of Eq. (2) one has to add the contribution $\tau_{\mu\nu}/2$ of the stress-energy tensor of the scalar field σ, which is

$$\tau_{\mu\nu} = \frac{16\pi\mathcal{F}'(y)}{\jmath}(\sigma_{,\mu}\sigma_{,\nu} - 2u^\mu\sigma_{,\mu}u_{(\mu}\sigma_{,\nu)}) - g_{\mu\nu}\frac{8\pi\mathcal{F}(y)}{\jmath^2\ell^2}, \quad (79)$$

where $y = \jmath\ell^2 j^{\mu\nu}\sigma_{,\mu}\sigma_{,\nu}$ and $\mathcal{F}'(y) = d\mathcal{F}(y)/dy$. Second, one has to add $-\frac{8\pi}{\jmath}\mathcal{F}'(y)u^\nu\sigma_{,\nu}g^{\mu\rho}\sigma_{,\rho}$ to the right-hand side of Eq. (3). Finally, the equations of motion for the scalar field σ are

$$\nabla_\nu[\mathcal{F}'(y)j^{\mu\nu}\sigma_{,\mu}] = 0. \quad (80)$$

Another important difference between Einstein-æther theory and the generalized TeVeS theory is that there are two metric tensors in the latter. The first metric $g_{\mu\nu}$ appearing in the actions (1) and (78) is called the "Einstein metric." The second metric $\tilde{g}_{\mu\nu} = e^{-2\sigma}g_{\mu\nu} - 2u_\mu u_\nu\sinh(2\sigma)$ is the physical metric, and the matter fields ψ_m minimally couple to this metric, i.e., the matter action is symbolically given by

$$S'_m = \int \mathrm{d}^4\sqrt{-\tilde{g}}\mathcal{L}(\tilde{g}_{\mu\nu}, \psi_m, \tilde{\nabla}_\mu\psi_m), \quad (81)$$

where $\tilde{\nabla}_\mu$ is the covariant derivative compatible with $\tilde{g}_{\mu\nu}$. Therefore, a neutral test particle travels on the geodesic determined by $\tilde{g}_{\mu\nu}$ in free fall. In general, the geodesics of $g_{\mu\nu}$ differ from those defined by $\tilde{g}_{\mu\nu}$, unless $\sigma = 0$.

A. Gravitational-wave solutions

In this work we find the GW solutions in the flat spacetime background. The background solution

$$g_{\mu\nu} = \eta_{\mu\nu}, \qquad u^\mu = \underline{u}^\mu, \qquad \sigma = \sigma_0 \quad (82)$$

(where σ_0 is a constant) requires that $\mathcal{F}(0) = 0$. Now, we perturb $g_{\mu\nu}$ and u^μ according to Eq. (7), and the scalar field σ is perturbed in the following way:

$$\sigma = \sigma_0 + \varsigma. \quad (83)$$

The linearized Einstein equation and the vector equation take the exact same forms as in Einstein-æther theory, which have been solved in Sec. II A. The linearized scalar equation is

$$\partial_\nu[\mathcal{F}'(0)j_0^{\mu\nu}\varsigma_{,\mu}] = 0, \quad (84)$$

with $j_0^{\mu\nu} = \eta^{\mu\nu} - \underline{u}^\mu\underline{u}^\nu = \mathrm{diag}(-2,1,1,1)$. If one chooses the original form for $\mathcal{F}$ [30], $\mathcal{F}''(0)$ blows up. However, there are other choices for $\mathcal{F}$ as given in Ref. [63], such that $\mathcal{F}''(0)$ is finite [64]. Expanding the above relation (84) gives

$$-\ddot{\varsigma} + \frac{1}{2}\nabla^2\varsigma = 0, \quad (85)$$

so the scalar perturbation ς propagates at the speed $s_0 = 1/\sqrt{2}$. Therefore, a plane-wave solution propagating in the positive z direction is

$$\varsigma = \varsigma_0\cos[\omega(t - z/s_0)], \quad (86)$$

where ς_0 is the amplitude and ω is the angular frequency. The plane-wave solutions for the metric and the vector fields have been given in Eqs. (40)–(43).

Up to the linear order, the physical metric is thus

$$\tilde{g}_{00} = e^{2\sigma_0}(-1 + h_{00} - 2\varsigma), \quad (87)$$

$$\tilde{g}_{0j} = 2v^j\sinh(2\sigma_0), \quad (88)$$

$$\tilde{g}_{jk} = e^{-2\sigma_0}[\delta_{jk}(1 - 2\varsigma) + h_{jk}]. \quad (89)$$

Note that this metric is written in coordinates determined by the Einstein metric $g_{\mu\nu}$, and the gauge conditions $h_{0j} = 0$ and $\partial_j v^j = 0$ have been imposed. If one performs the coordinate transformation [26]

$$\tilde{x}^0 = e^{\sigma_0}x^0, \qquad \tilde{x}^j = e^{-\sigma_0}x^j, \quad (90)$$

the physical metric becomes

$$\tilde{g}_{00} = -1 + h_{00} - 2\varsigma, \quad (91)$$

$$\tilde{g}_{0j} = 2v^j\sinh(2\sigma_0), \quad (92)$$

$$\tilde{g}_{jk} = \delta_{jk}(1 - 2\varsigma) + h_{jk}. \quad (93)$$

Note that all of the fields on the right-hand side in the above expressions are written as functions of $\tilde{x}^0$ and $\tilde{x}^j$ implicitly. In this coordinate system, the speeds become

$$\tilde{s}_g^2 = \frac{e^{-4\sigma_0}}{1 - c_{13}}, \quad (94)$$

$$\tilde{s}_v^2 = e^{-4\sigma_0}\frac{c_1 - c_1^2/2 + c_3^2/2}{c_{14}(1-c_{13})}, \tag{95}$$

$$\tilde{s}_s^2 = \frac{e^{-4\sigma_0}c_{123}(2-c_{14})}{c_{14}(1-c_{13})(2+2c_2+c_{123})}, \tag{96}$$

$$\tilde{s}_0^2 = \frac{e^{-4\sigma_0}}{2}. \tag{97}$$

Again, the speeds are not necessarily 1, and are generally different from one another. When all speeds are 1, the following conditions should be satisfied:

$$\sigma_0 = -\frac{\ln 2}{4}, \qquad c_1 = c_4 - \frac{1}{2},$$
$$c_3 = -c_4 - \frac{1}{2}, \qquad c_2 = \frac{1}{2(1-2c_4)}. \tag{98}$$

However, a negative σ_0 is not acceptable in this theory [66].

In total there are six d.o.f.: in addition to those that resemble the five d.o.f. in Einstein-æther theory, there is one more scalar d.o.f., σ. Note that there are two scalar d.o.f., σ and Ω, in this theory. All of these d.o.f. will affect the polarization content of GWs in the generalized TeVeS theory. The polarization content is obtained by calculating the linearized geodesic deviation equation $\ddot{\tilde{x}}^j = -\tilde{R}_{\tilde{t}\tilde{j}\tilde{t}\tilde{k}}\tilde{x}^k$, where $\tilde{R}_{\tilde{t}\tilde{j}\tilde{t}\tilde{k}}$ is the linearized Riemann tensor calculated using the physical metric $\tilde{g}_{\mu\nu}$. There are six polarization states in the generalized TeVeS theory: the plus polarization $\hat{P}_+ = -\tilde{R}_{\tilde{t}\tilde{x}\tilde{t}\tilde{x}} + \tilde{R}_{\tilde{t}\tilde{y}\tilde{t}\tilde{y}} = \ddot{h}_+$ and the cross polarization $\hat{P}_\times = \tilde{R}_{\tilde{t}\tilde{x}\tilde{t}\tilde{y}} = -\ddot{h}_\times$; the vector-$x$ polarization $\hat{P}_{xz} = \tilde{R}_{\tilde{t}\tilde{x}\tilde{t}\tilde{z}} = -\{c_{13}(1+2\sinh[2\sigma_0)] - 2\sinh(2\sigma_0)\}\ddot{v}_1/[2(1-c_{13})\tilde{s}_v]$, and the vector-$y$ polarization $\hat{P}_{yz} = \tilde{R}_{\tilde{t}\tilde{x}\tilde{t}\tilde{y}} = -\{c_{13}[1+2\sinh(2\sigma_0)] - 2\sinh(2\sigma_0)\}\ddot{v}_2/[2(1-c_{13})\tilde{s}_v]$; the transverse breathing polarization $\hat{P}_b = \tilde{R}_{\tilde{t}\tilde{x}\tilde{t}\tilde{x}} + \tilde{R}_{\tilde{t}\tilde{y}\tilde{t}\tilde{y}} = -c_{14}\ddot{\phi} + 2\ddot{\varsigma}$, and the longitudinal polarization

$$\hat{P}_l = \tilde{R}_{\tilde{t}\tilde{z}\tilde{t}\tilde{z}} = \left[\frac{(c_{14}-2c_{13})}{2(c_{13}-1)\tilde{s}_s^2} - \frac{c_{14}}{2}\right]\ddot{\phi} + \left(1 + \frac{1}{\tilde{s}_0^2}\right)\ddot{\varsigma}.$$

Therefore, the scalar d.o.f., ϕ and ς, excite two mixed states of $\hat{P}_b$ and $\hat{P}_l$. As in Einstein-æther theory, none of the Newman-Penrose variables vanish in general.

B. Discussion on the constraints

Sagi calculated the post-Newtonian parameters for the generalized TeVeS theory [66], and α_1 and α_2 are given in Eqs. (46)–(48) in Ref. [66], which are too complicated to be reproduced here. In her equations, $K = (c_1 - c_3)/2$, $K_+ = c_{13}/2$, $K_2 = c_2$, and $K_4 = -c_4$. She also found that

$$G = G_{\rm N}\frac{4\pi(2-c_{14})}{8\pi + \jmath(2-c_{14})}, \tag{99}$$

which should be positive (where $G_{\rm N}$ is Newton's constant). Using the expressions for α_1 and α_2, one can solve for $\jmath$ and c_2 in terms of σ_0, c_j ($j \neq 2$), and the α's. Note that α_1 and α_2 are not necessarily set to zero in the following discussion.

Next, the observations of GW170817 and GRB 170817A set bounds on the propagation speed of the tensor mode. The above discussion shows that there are four different speeds for different polarizations. Here, we set $\tilde{s}_g = 1 + \delta$ with $-3\times10^{-15} < \delta < 7\times10^{-16}$. This is the third constraint for this theory, and it relates σ_0 to c_{13}. Therefore, the parameter space reduces to three dimensions, conveniently parametrized by c_1, c_3, and c_4.

In addition, the MOND effects should not be too large in the Solar System, which requires that $\jmath$ is of the order of 0.01 [30,66]. Finally, by studying the neutron star and black hole solutions, the authors of Refs. [67–69] set a new bound, i.e., $c_{14} \lesssim 1$. With these constraints and bounds, one can scan the reduced parameter space to search for the parameter ranges such that all speeds are of the order of unity. The strategy is given below:

(1) Start with a relatively larger reduced parameter space S_0, i.e., $-10 < c_1, c_3, c_4 < 10$, and search for the subspace S_1 such that $\tilde{s}_v$ and $\tilde{s}_s$ are smaller than an upper bound v_0 (say, 10^{13}) with a common step size $\Delta^{(0)} = 20/N$, where N is an integer. In this search, all of the constraints and bounds should be taken into account.
(2) If such a subspace S_1 is found, one proceeds to the next iteration. In this iteration, the reduced parameter space is S_1 and the step size for c_i is given by $\Delta_i^{(1)} = \delta c_i/N (i = 1, 3, 4)$, where δc_i is the difference between the maximum and minimum values of c_i that define S_1. The new speed bound v_1 is also updated, given by the minimum speed $\tilde{s}_v$ or $\tilde{s}_s$ found in the previous iteration.
(3) If such a subspace S_1 cannot be found, the iteration terminates.

One repeats the above steps until one cannot find a subspace S_n such that $\tilde{s}_v, \tilde{s}_s < v_n$ in this subspace after n iterations. In order to avoid the influence of the step sizes on the final result, one can vary N. It turns out that one cannot find such a subspace in which $\tilde{s}_v$ and $\tilde{s}_s$ are both of the order of unity, while all of the constraints and bounds are satisfied simultaneously. This can be understood roughly by expressing $\tilde{s}_v$, $\tilde{s}_s$ in terms of $\tilde{s}_g$ with $\alpha_1 = \alpha_2 = 0$,

$$\tilde{s}_v^2 = \frac{\tilde{s}_g^2}{2}\frac{2c_1 - c_1^2 + c_3^2}{c_{14}} \tag{100}$$

$$\approx \frac{1}{2}\frac{2c_1 - c_1^2 + c_3^2}{c_{14}}, \tag{101}$$

$$\tilde{s}_s^2 = \frac{4\tilde{s}_g^2}{3}\left[1 - \frac{c_{14}}{2(1-\tilde{s}_g^{-2})}\right]^2 \frac{\tilde{s}_v^2}{2-c_{14}} \approx \frac{4}{3}(1-4\delta^{-1}c_{14})^2 \frac{\tilde{s}_v^2}{2-c_{14}}. \quad (102)$$

At the same time, $\jmath$ can be approximated as

$$\jmath \approx \frac{4\pi c_{14}}{c_{14}-2} + 8\pi\delta, \quad (103)$$

so c_{14} is of the order of 10^{-2}. If $\tilde{s}_v$ is of the order of unity and δ takes the largest value $|\delta| \sim 10^{-15}$, $\tilde{s}_s$ is of order 10^{13}! Any attempt to reduce $\tilde{s}_s$ to be of the order of unity while keeping $\tilde{s}_v \sim 1$ fails. A more serious problem is that $\tilde{s}_s$ blows up as δ approaches 0, as one can check from Eq. (102). On the other hand, one may also consider simply setting $\delta = 0$ (i.e., $\tilde{s}_g = 1$) without requiring $\alpha_1 = \alpha_2 = 0$. In this case, one obtains that

$$\jmath = \frac{8\pi(\alpha_1 + 4c_{14})}{(8+\alpha_1)(c_{14}-2)}, \quad (104)$$

which can be solved for c_{14}. At the same time, one finds that

$$\tilde{s}_s^2 = \frac{(8+\alpha_1)c_{14}}{7\alpha_1(2-c_{14})} = -\frac{(\alpha_1+8)\jmath + 4\pi\alpha_1}{28\pi\alpha_1} \sim 10^2. \quad (105)$$

So the scalar field ϕ will still propagate at a large (although not necessarily infinite) speed, which might lead to a faster decay of the orbit of a binary system.

A very large speed might lead to the strong coupling problem, and the scalar mode ϕ might not be excited. In this case, one has to integrate out this mode and then apply the experimental constraints to the resulting theory. In order to examine whether the strong coupling problem arises, one needs to expand the action up to the cubic order in the scalar perturbations, and calculate all of the coefficients of the terms in the cubic action after canonically normalizing the scalar d.o.f. The resulting cubic Lagrangian is very complicated and will not be presented here. It shows that the strong coupling problem exists in some parameter subspaces. For example, Fig. 7 shows the allowed parameter subspaces, which were obtained by scanning the parameter space. The gray areas represent the parameter subspaces in which the strong coupling problem does not exist, while the dark gray areas represent the parameter subspaces in which the strong coupling problem does exist. So in these dark gray areas the above analysis on the scalar mode cannot be applied. These allowed parameter subspaces depend on δ and the α_i's. However, the changes due to varying δ and the α_i's are very small. So the generalized TeVeS theory is excluded due to the large or even infinite speed $\tilde{s}_s$, given the speed limits on the tensor GW mode, in the parameter space where the strong coupling problem does not exist.

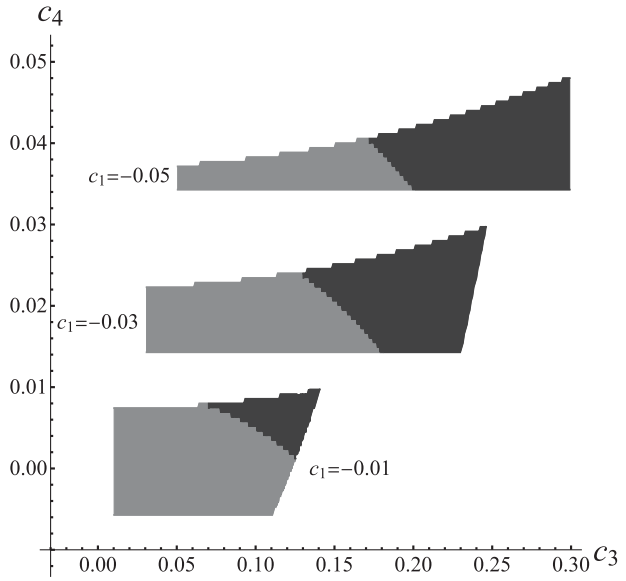

FIG. 7. Parameter subspaces (colored areas) allowed by the experimental constraints. There are three chunks of allowed parameter subspaces corresponding to different values of c_1. Each allowed region is divided into two pieces. The gray areas represent the parameter subspaces in which the strong coupling problem does not exist, while the dark gray areas represent the parameter subspaces in which the strong coupling problem does exist. (The jagged boundaries are due to the finite step size used in the scanning.)

IV. CONCLUSION

In this work, we discussed the linear GW solutions around the flat spacetime background and the polarization contents of Einstein-æther theory and the generalized TeVeS theory. It turns out that both theories predict the existence of tensor, vector, and scalar GWs, each propagating with different speeds generally different from 1. In obtaining the GW solutions, we used the gauge-invariant variables to help separate the physical d.o.f. There are five polarization states in Einstein-æther theory, while the generalized TeVeS theory predicts the existence of six polarization states. The transverse breathing mode is mixed with the longitudinal mode to form a single state for the scalar polarization in Einstein-æther theory. The two scalar polarizations in the generalized TeVeS theory are two mixed states of the transverse breathing and longitudinal modes. In addition, the possible experimental tests of the polarizations in Einstein-æther theory have been considered by using the cross-correlation functions of PTAs for the various polarizations together with the speed bounds on

GWs set by the observations of GW170817 and GRB 170817A. We found that the cross-correlation functions for different polarizations look very similar to each other in some parameter regions, and this means that it will be difficult for PTAs to identify the polarizations. However, in the parameter regions with $c_{13} = 0$, the cross-correlation function for the extra polarization (i.e., the scalar one) is rather different from the tensor one, so it is possible to use PTAs to identify the polarizations. The implication of the speed bounds on GWs for the generalized TeVeS theory was also considered. The very tight speed bound drives $\tilde{s}_s$ to be much greater than 1, which is unnatural. It was also checked that the strong coupling problem does not exist in some parameter subspaces by taking into account all experimental constraints. So the generalized TeVeS theory is excluded by the speed bounds on GWs in these parameter subspaces.

ACKNOWLEDGMENTS

We thank Ted Jacobson for constructive discussions. This research was supported in part by the Major Program of the National Natural Science Foundation of China under Grant No. 11690021 and the National Natural Science Foundation of China under Grant No. 11475065.

APPENDIX: CALCULATING THE CROSS-CORRELATION FUNCTIONS

In this appendix we present the method to calculate the cross-correlation functions for the scalar, vector, and tensor polarizations in Einstein-æther theory.

1. Scalar cross-correlation function

The relative frequency shift caused by the monochromatic scalar GW is given by the first line in Eq. (68),

$$\frac{f_e - f_r}{f_r} = \frac{(c_{14} - 2c_{13})(\hat{k}\cdot\hat{n})^2 + s_s^2 c_{14}(1 - c_{13})}{2(1 - c_{13})s_s(s_s + \hat{k}\cdot\hat{n})} \times [\phi(t, 0) - \phi(t - L/s_s, L\hat{n})]. \tag{A1}$$

Let the stochastic GW background be described by Eq. (69); thus, the timing residual is

$$R(T) = \int_{-\infty}^{\infty}\frac{d\omega}{2\pi}\int d^2\hat{k}\left\{I_s(\hat{k},\hat{n})\varphi(\omega,\hat{k})\frac{e^{i\omega T} - 1}{i\omega} \times [1 - e^{-i\omega L(1+\hat{k}\cdot\hat{n}/s_s)}]\right\}, \tag{A2}$$

where

$$I_s(\hat{k},\hat{n}) = \frac{(c_{14} - 2c_{13})(\hat{k}\cdot\hat{n})^2 + s_s^2 c_{14}(1 - c_{13})}{2(1 - c_{13})s_s(s_s + \hat{k}\cdot\hat{n})}. \tag{A3}$$

Now, consider the correlation between two pulsars a and b which are at positions $\vec{x}_a = L_1\hat{n}_1$ and $\vec{x}_b = L_2\hat{n}_2$, respectively. Let $\theta = \arccos(\hat{n}_1\cdot\hat{n}_2)$ be the angular separation. With the help of Eq. (74), the cross-correlation function between pulsars a and b is obtained as

$$C_s(\theta) = \langle R_a(T)R_b(T)\rangle = \int_0^{\infty}\frac{d\omega}{2\pi^2}\int d^2\hat{k}\frac{|\varphi_c(\omega)|^2}{\omega^3}I_s(\hat{k},\hat{n}_a)I_s(\hat{k},\hat{n}_b)\mathcal{P}_s, \tag{A4}$$

where $\mathcal{P}_s = 1 - \cos\Delta_1 - \cos\Delta_2 + \cos(\Delta_1 - \Delta_2)$ with $\Delta_j = \omega L_j(1 + \hat{k}\cdot\hat{n}_j/s_s)$ $(j = 1, 2)$. In obtaining this result, one also averages over T, as implied by the ensemble average [56].

If the speed s_s takes the values listed in the third row of Table I, there will be no poles in the integrand of Eq. (A4). This is because the denominator of the integrand has a factor $(s_s + \hat{k}\cdot\hat{n}_1)(s_s + \hat{k}\cdot\hat{n}_2)$, and $\hat{k}\cdot\hat{n}_j \geq -1$, so the denominator never vanishes. We can approximate $\mathcal{P}_s = 1$ whenever $\theta \neq 0$, since pulsars are located at far enough distances so that the cosines in $\mathcal{P}_s$ oscillate fast enough and they can be ignored during the integration. If $\theta = 0$, the autocorrelation is considered by setting $\hat{n}_1 = \hat{n}_2$ and $L_1 = L_2$, and $\mathcal{P}_s \approx 2$. In contrast, when null GWs are considered, the integrand [see Eqs. (A36) and (A39) in Ref. [56]] has at least one pole, so $\mathcal{P}_s$ cannot be simply approximated as 1 or 2.

Now, one can carry out the integration by letting

$$\hat{n}_1 = (0, 0, 1), \tag{A5}$$

$$\hat{n}_2 = (\sin\theta, 0, \cos\theta), \tag{A6}$$

with the assumption that the stochastic GW background is isotropic. Take

$$\hat{k} = (\sin\theta_g\cos\phi_g, \sin\theta_g\sin\phi_g, \cos\theta_g), \tag{A7}$$

and so

$$\Delta_1 = (\omega + k\cos\theta_g)L_1, \tag{A8}$$

$$\Delta_2 = [\omega + k(\sin\theta_g\cos\phi_g\sin\theta + \cos\theta_g\cos\theta)]L_2. \tag{A9}$$

The cross correlation at $\theta \neq 0$ is given by

$$C_s(\theta) = \int \mathrm{d}\phi_g \mathrm{d}\theta_g [I_s(\hat{k},\hat{n}_1) I_s(\hat{k},\hat{n}_2) \sin\theta_g] \times \int_0^\infty \mathrm{d}\omega \frac{|\varphi_c(\omega)|^2}{2\pi^2\omega^3}, \tag{A10}$$

and the autocorrelation is

$$C_s(0) = 2\int \mathrm{d}\phi_g \mathrm{d}\theta_g [I_s(\hat{k},\hat{n}_1) I_s(\hat{k},\hat{n}_1) \sin\theta_g] \times \int_0^\infty \mathrm{d}\omega \frac{|\varphi_c(\omega)|^2}{2\pi^2\omega^3}. \tag{A11}$$

We define the so-called normalized cross correlation $\zeta(\theta) = C_s(\theta)/C_s(0)$; then, the frequency dependence is canceled out, so $\zeta(\theta)$ is independent of the power-law index α.

2. Vector cross-correlation function

The relative frequency shift caused by a monochromatic vector GW is

$$\frac{f_e - f_r}{f_r} = -\frac{c_{13}\hat{k}\cdot\hat{n}}{(1-c_{13})(s_v + \hat{k}\cdot\hat{n})} \times [\hat{n}\cdot\vec{v}(t,0) - \hat{n}\cdot\vec{v}(t - L/s_v, L\hat{n})]. \tag{A12}$$

Now, we switch off $\mu_{\tilde{2}}(\omega,\hat{k})$, as the two modes $\mu_{\tilde{1}}(\omega,\hat{k})$ and $\mu_{\tilde{2}}(\omega,\hat{k})$ have an equal footing. The timing residual caused by the stochastic vector GW background is given by

$$R(T) = \int_{-\infty}^{\infty}\frac{\mathrm{d}\omega}{2\pi}\int \mathrm{d}^2\hat{k}\left\{ I_v(\hat{k},\hat{n})\mu_{\tilde{1}}(\omega,\hat{k}) \times \frac{e^{i\omega T}-1}{i\omega}[1 - e^{-i\omega L(1+\hat{k}\cdot\hat{n}/s_v)}]\right\}, \tag{A13}$$

where

$$I_v(\hat{k},\hat{n}) = -\frac{c_{13}(\hat{k}\cdot\hat{n})(\hat{n}\cdot\hat{e}_{\tilde{1}})}{(1-c_{13})(s_v+\hat{k}\cdot\hat{n})}. \tag{A14}$$

So the cross correlation is

$$C_v(\theta) = \int_0^\infty \frac{\mathrm{d}\omega}{2\pi^2}\int \mathrm{d}^2\hat{k}\frac{|\mu_{\tilde{1}}^c(\omega)|^2}{\omega^3} I_v(\hat{k},\hat{n}_1) I_v(\hat{k},\hat{n}_2)\mathcal{P}_v, \tag{A15}$$

where $\mathcal{P}_v$ can be obtained by replacing s_s in $\mathcal{P}_s$ with s_v. With $\hat{k}$, $\hat{n}_1$, and $\hat{n}_2$ given by Eqs. (A7), (A5), and (A6), $\hat{e}_{\tilde{1}}$ and $\hat{e}_{\tilde{2}}$ are

$$\hat{e}_{\tilde{1}} = (\cos\psi\cos\theta_g\cos\phi_g - \sin\psi\sin\phi_g, \cos\psi\cos\theta_g\sin\phi_g + \sin\psi\cos\phi_g, -\cos\psi\sin\theta_g), \tag{A16}$$

$$\hat{e}_{\tilde{2}} = (-\sin\psi\cos\theta_g\cos\phi_g - \cos\psi\sin\phi_g, \cos\psi\cos\phi_g - \sin\psi\cos\theta_g\sin\phi_g, \sin\psi\sin\theta_g). \tag{A17}$$

Note that if s_v takes the values in the second row in Table I, the integrand of Eq. (A15) has no poles either. So one approximates $\mathcal{P}_v$ to be 1 when $\theta \neq 0$, and 2 when $\theta = 0$. The normalized cross-correlation function $\zeta(\theta) = C_v(\theta)/C_v(0)$ can thus be numerically calculated, and it is easy to see that $\zeta(\theta)$ is independent of the power-law index α.

3. Tensor cross-correlation function

For the tensor GWs, the relative frequency shift is

$$\frac{f_e - f_r}{f_r} = \frac{s_g\hat{n}^j\hat{n}^k}{2(s_g+\hat{k}\cdot\hat{n})}[h_{jk}^{\mathrm{TT}}(t,0) - h_{jk}^{\mathrm{TT}}(t - L/s_g, L\hat{n})]. \tag{A18}$$

As stated in Sec. II D, this expression takes exactly the same form as in GR as long as $s_g = 1$. If $s_g \neq 1$, this form resembles those for the massive GWs discussed in Refs. [57,58], where the GW speed depends on the angular frequency through the dispersion relation.

Let us consider the cross correlation due to the plus polarization. The timing residual of TOA is given by

$$R(T) = \int_{-\infty}^{\infty}\frac{\mathrm{d}\omega}{2\pi}\int \mathrm{d}^2\hat{k}\left\{ I_g(\hat{k},\hat{n}) h_+(\omega,\hat{k}) \times \frac{e^{i\omega T}-1}{i\omega}[1 - e^{-i\omega L(1+\hat{k}\cdot\hat{n}/s_g)}]\right\}, \tag{A19}$$

where

$$I_g(\hat{k},\hat{n}) = \frac{s_g\hat{n}^j\hat{n}^k\epsilon_{jk}^+}{2(s_g+\hat{k}\cdot\hat{n})}. \tag{A20}$$

The cross correlation is thus

$$C_g(\theta) = \int_0^\infty \frac{\mathrm{d}\omega}{8\pi}\int \mathrm{d}^2\hat{k}\frac{|h_c^+(\omega)|^2}{\omega^3} I_g(\hat{k},\hat{n}_1) I_g(\hat{k},\hat{n}_2)\mathcal{P}_g, \tag{A21}$$

in which $\mathcal{P}_g$ takes a similar form as $\mathcal{P}_s$ with s_s replaced by s_g. Let $s_g = 1 + 7\times 10^{-16}$, so that the integrand of Eq. (A21) has no poles, and the integration can be easily done by setting $\mathcal{P}_g = 1$ for $\theta \neq 0$ and setting $\mathcal{P}_g = 2$ for $\theta = 0$. The normalized cross-correlation function $\zeta(\theta) = C_g(\theta)/C_g(0)$ can be calculated numerically.

[1] B. P. Abbott *et al.* (Virgo and LIGO Scientific Collaborations), Phys. Rev. Lett. **116**, 061102 (2016).
[2] B. P. Abbott *et al.* (Virgo and LIGO Scientific Collaborations), Phys. Rev. Lett. **116**, 241103 (2016).
[3] B. P. Abbott *et al.* (Virgo and LIGO Scientific Collaborations), Phys. Rev. Lett. **118**, 221101 (2017).
[4] B. P. Abbott *et al.* (Virgo and LIGO Scientific Collaborations), Phys. Rev. Lett. **119**, 141101 (2017).
[5] B. P. Abbott *et al.* (Virgo and LIGO Scientific Collaborations), Phys. Rev. Lett. **119**, 161101 (2017).
[6] B. P. Abbott *et al.* (Virgo and LIGO Scientific Collaborations), Astrophys. J. **851**, L35 (2017).
[7] A. Goldstein *et al.*, Astrophys. J. **848**, L14 (2017).
[8] V. Savchenko *et al.*, Astrophys. J. **848**, L15 (2017).
[9] M. Kramer and D. J. Champion, Classical Quantum Gravity **30**, 224009 (2013).
[10] G. Hobbs *et al.*, Classical Quantum Gravity **27**, 084013 (2010).
[11] M. A. McLaughlin, Classical Quantum Gravity **30**, 224008 (2013).
[12] G. Hobbs, Classical Quantum Gravity **30**, 224007 (2013).
[13] C. J. Moore, R. H. Cole, and C. P. L. Berry, Classical Quantum Gravity **32**, 015014 (2015).
[14] P. A. Seoane *et al.* (eLISA Collaboration), arXiv:1305.5720.
[15] J. Luo *et al.* (TianQin Collaboration), Classical Quantum Gravity **33**, 035010 (2016).
[16] S. Kawamura *et al.*, Classical Quantum Gravity **28**, 094011 (2011).
[17] P. W. Graham, J. M. Hogan, M. A. Kasevich, S. Rajendran, and R. W. Romani, arXiv:1711.02225.
[18] D. M. Eardley, D. L. Lee, and A. P. Lightman, Phys. Rev. D **8**, 3308 (1973).
[19] C. M. Will, Living Rev. Relativity **17**, 4 (2014).
[20] D. Liang, Y. Gong, S. Hou, and Y. Liu, Phys. Rev. D **95**, 104034 (2017).
[21] S. Hou, Y. Gong, and Y. Liu, arXiv:1704.01899.
[22] Y. Gong and S. Hou, EPJ Web Conf. **168**, 01003 (2018).
[23] T. Jacobson and D. Mattingly, Phys. Rev. D **64**, 024028 (2001).
[24] T. Jacobson and D. Mattingly, Phys. Rev. D **70**, 024003 (2004).
[25] M. D. Seifert, Phys. Rev. D **76**, 064002 (2007).
[26] E. Sagi, Phys. Rev. D **81**, 064031 (2010).
[27] B. P. Abbott *et al.* (Virgo, Fermi-GBM, INTEGRAL, and LIGO Scientific Collaborations), Astrophys. J. **848**, L13 (2017).
[28] P. M. Chesler and A. Loeb, Phys. Rev. Lett. **119**, 031102 (2017).
[29] T. G. Złośnik, P. G. Ferreira, and G. D. Starkman, Phys. Rev. D **75**, 044017 (2007).
[30] J. D. Bekenstein, Phys. Rev. D **70**, 083509 (2004); **71**, 069901(E) (2005).
[31] M. Milgrom, Astrophys. J. **270**, 365 (1983).
[32] M. Milgrom, Astrophys. J. **270**, 371 (1983).
[33] M. Milgrom, Astrophys. J. **270**, 384 (1983).
[34] T. Baker, E. Bellini, P. G. Ferreira, M. Lagos, J. Noller, and I. Sawicki, Phys. Rev. Lett. **119**, 251301 (2017).
[35] A. Pasqua, S. Chattopadhyay, D. Momeni, M. Raza, R. Myrzakulov, and M. Faizal, J. Cosmol. Astropart. Phys. 04 (2017) 015.
[36] E. E. Flanagan and S. A. Hughes, New J. Phys. **7**, 204 (2005).
[37] E. Newman and R. Penrose, J. Math. Phys. (N.Y.) **3**, 566 (1962); **4**, 998(E) (1963).
[38] D. M. Eardley, D. L. Lee, A. P. Lightman, R. V. Wagoner, and C. M. Will, Phys. Rev. Lett. **30**, 884 (1973).
[39] B. Z. Foster and T. Jacobson, Phys. Rev. D **73**, 064015 (2006).
[40] E. Poisson and C. M. Will, *Gravity: Newtonian, Post-Newtonian, Relativistic* (Cambridge University Press, Cambridge, England, 2014).
[41] P. C. C. Freire, N. Wex, G. Esposito-Farèse, J. P. W. Verbiest, M. Bailes, B. A. Jacoby, M. Kramer, I. H. Stairs, J. Antoniadis, and G. H. Janssen, Mon. Not. R. Astron. Soc. **423**, 3328 (2012).
[42] L. Shao, R. N. Caballero, M. Kramer, N. Wex, D. J. Champion, and A. Jessner, Classical Quantum Gravity **30**, 165019 (2013).
[43] I. I. Shapiro, Rev. Mod. Phys. **71**, S41 (1999).
[44] S. M. Carroll and E. A. Lim, Phys. Rev. D **70**, 123525 (2004).
[45] T. Jacobson, *Proc. Sci.*, QG-PH2007 (2007) 020, arXiv: 0801.1547.
[46] J. W. Elliott, G. D. Moore, and H. Stoica, J. High Energy Phys. 08 (2005) 066.
[47] K. Yagi, D. Blas, N. Yunes, and E. Barausse, Phys. Rev. Lett. **112**, 161101 (2014).
[48] K. Yagi, D. Blas, E. Barausse, and N. Yunes, Phys. Rev. D **89**, 084067 (2014); **90**, 069901(E) (2014); **90**, 069902(E) (2014).
[49] J. Oost, S. Mukohyama, and A. Wang, arXiv:1802.04303.
[50] J. P. W. Verbiest *et al.*, Mon. Not. R. Astron. Soc. **400**, 951 (2009).
[51] F. B. Estabrook and H. D. Wahlquist, Gen. Relativ. Gravit. **6**, 439 (1975).
[52] M. V. Sazhin, Sov. Astron. **22**, 36 (1978).
[53] S. L. Detweiler, Astrophys. J. **234**, 1100 (1979).
[54] R. W. Hellings and G. S. Downs, Astrophys. J. **265**, L39 (1983).
[55] F. A. Jenet, G. B. Hobbs, K. J. Lee, and R. N. Manchester, Astrophys. J. **625**, L123 (2005).
[56] K. J. Lee, F. A. Jenet, and R. H. Price, Astrophys. J. **685**, 1304 (2008).
[57] K. Lee, F. A. Jenet, R. H. Price, N. Wex, and M. Kramer, Astrophys. J. **722**, 1589 (2010).
[58] K. J. Lee, Classical Quantum Gravity **30**, 224016 (2013).
[59] S. J. Chamberlin and X. Siemens, Phys. Rev. D **85**, 082001 (2012).
[60] N. Yunes and X. Siemens, Living Rev. Relativity **16**, 9 (2013).
[61] J. Gair, J. D. Romano, S. Taylor, and C. M. F. Mingarelli, Phys. Rev. D **90**, 082001 (2014).
[62] J. R. Gair, J. D. Romano, and S. R. Taylor, Phys. Rev. D **92**, 102003 (2015).
[63] C. Skordis, Classical Quantum Gravity **26**, 143001 (2009).
[64] For example, one can set $\mu_a = 1$ and $n = 3$ in Eq. (38) in Refs. [63,65], so that $\mathcal{F}'(y) \approx \mu_0(3 - \frac{64\pi\ell^2}{27\mu_0^2}y) + O(y^2)$.
[65] F. Bourliot, P. G. Ferreira, D. F. Mota, and C. Skordis, Phys. Rev. D **75**, 063508 (2007).
[66] E. Sagi, Phys. Rev. D **80**, 044032 (2009).
[67] E. Sagi and J. D. Bekenstein, Phys. Rev. D **77**, 024010 (2008).
[68] P. D. Lasky, H. Sotani, and D. Giannios, Phys. Rev. D **78**, 104019 (2008).
[69] P. D. Lasky, Phys. Rev. D **80**, 081501 (2009).